

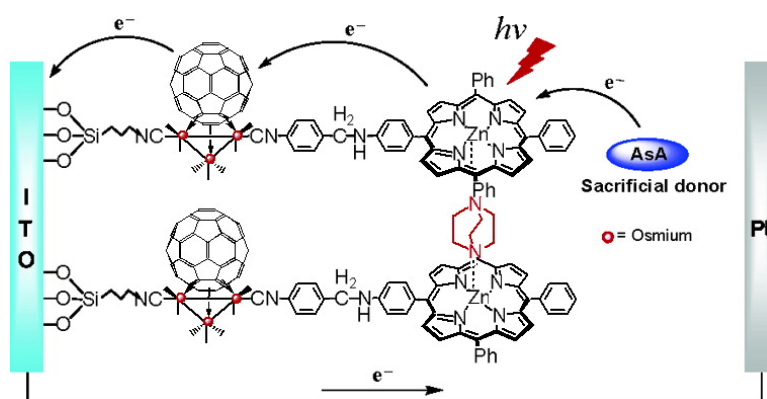
Communication

Unusually High Performance Photovoltaic Cell Based on a [60]Fullerene Metal Cluster–Porphyrin Dyad SAM on an ITO Electrode

Youn-Jaung Cho, Tae Kyu Ahn, Hyunjoon Song, Kil Suk Kim, Chang Yeon Lee, Won Seok Seo, Kwangyeol Lee, Seong Keun Kim, Dongho Kim, and Joon T. Park

J. Am. Chem. Soc., **2005**, 127 (8), 2380-2381 • DOI: 10.1021/ja044847x • Publication Date (Web): 04 February 2005

Downloaded from <http://pubs.acs.org> on March 24, 2009



More About This Article

Additional resources and features associated with this article are available within the HTML version:

- Supporting Information
- Links to the 19 articles that cite this article, as of the time of this article download
- Access to high resolution figures
- Links to articles and content related to this article
- Copyright permission to reproduce figures and/or text from this article

[View the Full Text HTML](#)

Unusually High Performance Photovoltaic Cell Based on a [60]Fullerene Metal Cluster–Porphyrin Dyad SAM on an ITO Electrode

Youn-Jaung Cho,[†] Tae Kyu Ahn,^{‡,§} Hyunjoon Song,[†] Kil Suk Kim,[‡] Chang Yeon Lee,[†]
Won Seok Seo,[†] Kwangyeol Lee,[†] Seong Keun Kim,[§] Dongho Kim,^{*,‡} and Joon T. Park^{*,†}

National Research Laboratory, Department of Chemistry and School of Molecular Science (BK21), Korea Advanced Institute of Science and Technology, Daejeon 305-701, Korea, Center for Ultrafast Optical Characteristic Control and Department of Chemistry, Yonsei University, Seoul 120-749, Korea, and School of Chemistry, Seoul National University, Seoul 151-747, Korea

Received August 26, 2004; E-mail: joontpark@kaist.ac.kr; dongho@yonsei.ac.kr

Photoinduced electron transfer (ET) in donor–acceptor (D–A) molecular systems has received considerable attention for applications such as optoelectronics, photonics, sensors, and other nano-scale molecular devices.¹ Coupled with porphyrins and/or ferrocenes as electron donors, C₆₀-containing systems such as dyad and triad have recently been demonstrated as the most prominent photovoltaic devices in artificial photosynthetic cells.² The most intriguing characteristics of C₆₀ as an electron acceptor are that it accelerates photoinduced charge separation and slows down charge recombination in the ET process, mainly because of its relatively low-lying LUMO and small reorganization energy.³ Recently, we have reported that C₆₀–metal cluster complexes show remarkable stabilities in the reduced state and strong electronic communication between C₆₀ and metal cluster centers.⁴

Self-assembled monolayers (SAMs) and multilayer thin films with potential gradients have proven to be promising in mimicking the natural photosynthetic apparatus and fabricating efficient photovoltaic cells.⁵ Herein we report the preparation of a novel C₆₀–porphyrin dyad structure Os₃(CO)₇(CNR)(CNR')(μ₃-η²:η²-C₆₀) (ZnP–C₆₀; R = (CH₂)₃Si(OEt)₃, R' = ZnP) (Scheme S1),⁶ in which a triosmium carbonyl cluster moiety links C₆₀ and a porphyrin unit and 3-(triethoxysilyl)propyl isocyanide is employed as a surface-anchoring ligand. Compound ZnP–C₆₀ forms an ideal SAM (abbreviated as (ZnP)–C₆₀/ITO; see the inset in Figure 1) with an almost full surface coverage on the ITO electrode in the presence of diazabicyclooctane (DABCO), which exhibits well-defined electrochemical responses and remarkably high photocurrent generation in C₆₀-based photovoltaic cells.

The UV/vis spectrum of (ZnP)–C₆₀/ITO shows that the characteristic Soret band becomes broader and the λ_{max} value of B bands is red-shifted by 11 nm relative to that of ZnP–C₆₀ in CH₂-Cl₂ (Figure 1). The broadening and bathochromic shift indicate moderate perturbation within SAMs mainly due to DABCO binding and porphyrin aggregates.⁷ The red shift of the B band implies that the axial DABCO binding to the d_{z²} orbitals of zinc lowers the porphyrin singlet excited state and also enhances the porphyrin surface coverage on ITO (vide infra).

The cyclic voltammogram (CV) of (ZnP)–C₆₀/ITO (Figure 2) reveals three well-resolved redox waves at –1.17, –1.47, and –1.92 V (E_{1/2}) with relative areas of 1:1:3.1. Importantly, the overall feature of CV of (ZnP)–C₆₀/ITO is similar to that of ZnP–C₆₀ in solution. The first and second waves are successive one-electron reductions localized on C₆₀. The third wave corresponds to an overlapped pattern of two-electron reduction of the C₆₀–triosmium

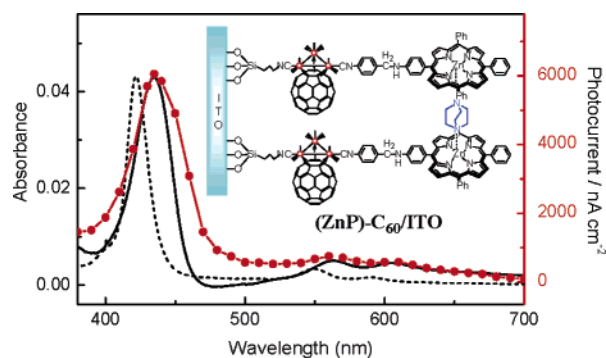


Figure 1. Absorption spectra of ZnP–C₆₀ (···) in CH₂Cl₂ and (ZnP)–C₆₀/ITO (—), and the action spectrum of (ZnP)–C₆₀/ITO/AsA/Pt (red line) with 0.96 mW cm^{–2} light at 100 mV bias vs Ag/AgCl. Inset shows the molecular structure of (ZnP)–C₆₀/ITO (the red atoms are osmium atoms, and carbonyl ligands are omitted for clarity).

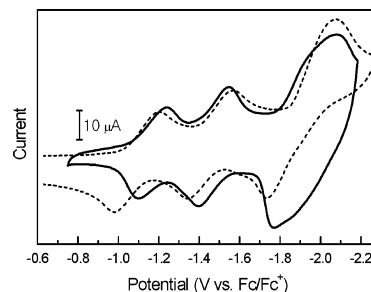


Figure 2. Cyclic voltammograms of ZnP–C₆₀ in chlorobenzene (···) and (ZnP)–C₆₀/ITO in CH₂Cl₂ (—) with 0.1 M Bu₄NPF₆ as an electrolyte at a scan rate of 0.5 V s^{–1}.

cluster moiety and one-electron reduction of the porphyrin moiety (Figure S1).⁶ Two successive waves are also observed at 0.29 and 0.48 V (E_{1/2}) for (ZnP)–C₆₀/ITO due to the first and second oxidations of the porphyrin moiety (Figure S2).⁶ The monolayer surface coverage (Γ) of (ZnP)–C₆₀/ITO is estimated to be 1.8 × 10^{–10} mol cm^{–2} from the integrated charge of the first reduction peak at –1.17 V, which is comparable to ~1.9 × 10^{–10} mol cm^{–2} for a closely packed monolayer of C₆₀.⁸ The coverage of (ZnP)–C₆₀/ITO is three times higher than that of ZnP–C₆₀/ITO (SAM without DABCO, 0.6 × 10^{–10} mol cm^{–2}, Figure S3⁶), which is consistent with the data in UV/vis spectra and AFM images (Figure S4).⁶ Well-ordered structural confinement via strong interaction of metalloporphyrin with a bifunctional base DABCO may be responsible for such high surface coverage.

Photocurrent measurements for SAMs were carried out using ascorbic acid (AsA) as a sacrificial electron donor by the typical reported procedures.^{2c,5d,6} A stable anodic photocurrent appears

[†] Korea Advanced Institute of Science and Technology.

[‡] Yonsei University.

[§] Seoul National University.

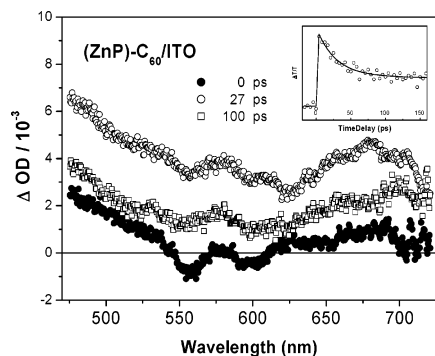


Figure 3. Transient absorption spectra of (ZnP)–C₆₀/ITO at 0 (●), 27 (□), and 100 (○) ps time delays with photoexcitation at 400 nm. Inset shows the transient absorption kinetic profiles at 430 nm.

immediately upon irradiation of the ITO electrode with 435 nm light (0.96 mW cm⁻²), and the response is reversibly repeated (Figure S5).⁶ The action spectrum of (ZnP)–C₆₀/ITO/AsA/Pt cell matches well with the absorption spectrum of (ZnP)–C₆₀/ITO in the 380–700 nm region (Figure 1), indicative of Zn(II)porphyrin as a photoactive sensitizer for the photocurrent generation. The anodic photocurrent increases in proportion to an increase of the positive bias of the ITO electrode (Figure S6).⁶ The quantum yields for ZnP–C₆₀/ITO/AsA/Pt and (ZnP)–C₆₀/ITO/AsA/Pt cells are estimated to be 10.4 and 19.5%, respectively, based on the number of photons absorbed by the chromophores. To the best of our knowledge, the present (ZnP)–C₆₀/ITO/AsA/Pt cell exhibits the highest quantum efficiency ever reported for molecular photovoltaic cells (dyad 6%,^{5c,d} triad 11%^{5d}), based on the covalently linked D–A dyad structure on ITO.

The fluorescence lifetimes of various SAMs were measured by using time-correlated single-photon counting technique with excitation at 420 nm (Figure S7 and Table S1).⁶ The fluorescence decay of SAM on the ITO surface was monitored at 605 nm corresponding to Zn(II)porphyrin emission. The fast components of fluorescence lifetimes of ZnP–C₆₀/ITO (12 ps) and (ZnP)–C₆₀/ITO (27 ps) are shorter than those of corresponding reference SAMs without C₆₀ such as ZnP–Os/ITO and (ZnP)–Os/ITO (52 and 66 ps, respectively).⁶ This observation implies a strong quenching of the porphyrin singlet excited state by the C₆₀ ligand via intramolecular electron transfer in C₆₀-containing SAMs. A slightly longer fluorescence lifetime of (ZnP)–C₆₀/ITO (27 ps) compared with that of ZnP–C₆₀/ITO (12 ps) may be attributed to the fact that the complexation of DABCO between the two Zn(II)porphyrins precludes aggregation with adjacent porphyrins. Furthermore, this structural confinement increases the donor–acceptor separation. The moderate fluorescence lifetimes of our SAMs, ZnP–C₆₀/ITO and (ZnP)–Os/ITO (Table S1),⁶ are believed to arise from self-quenching in aggregated porphyrins, based on previous results that the fluorescence lifetimes of ZnP reference molecules on ITO and slide glass are similar.^{5c} These fast ET processes in (ZnP)–C₆₀/ITO seem to be responsible for the high performance in photocurrent generation.

The femtosecond transient absorption decay profiles of ZnP–C₆₀/ITO and (ZnP)–C₆₀/ITO with excitation at 400 nm were also measured to confirm the intramolecular electron transfer from the porphyrin singlet excited state to C₆₀ on ITO. The ground-state bleaching recovery profiles of ZnP–C₆₀/ITO and (ZnP)–C₆₀/ITO at 430 nm could be fitted as double exponential decays, 12 and 92 ps and 27 ps and 2.4 ns (inset in Figure 3), respectively. The fast components are in good agreement with the fluorescence lifetimes

of ZnP–C₆₀/ITO (12 ps) and (ZnP)–C₆₀/ITO (27 ps). In addition, the transient absorption spectrum acquired at 27 ps time delay for (ZnP)–C₆₀/ITO reveals a broad absorption band in the 630–720 nm region and an absorption tail extending to 600 nm with apparent ground-state bleaching signals at 560 and 600 nm (Figure 3). The former is consistent with the spectral feature of porphyrin cation radical ZnP^{•+},⁹ and the latter corresponds to the characteristic absorption of the DABCO cation,¹⁰ in which both absorption increase and decay change at the same rate. This confirms the generation of [DABCO–ZnP]^{•+} with ca. 27 ps rise and a few hundred picosecond decay time. The positive charge can be distributed over both moieties, instead of being localized exclusively on ZnP or DABCO, which may lower the charge recombination rate leading to an increase in the photocurrent generation efficiency.⁹

In conclusion, we have successfully constructed highly ordered, nearly fully covered [60]fullerene metal cluster–porphyrin dyad SAM on the ITO surface with an aid of DABCO binding in (ZnP)–C₆₀/ITO, which leads to the unusually high photocurrent generation efficiency in the (ZnP)–C₆₀/ITO/AsA/Pt cell. We have provided direct spectroscopic evidence for the formation of [DABCO–ZnP]^{•+} in the photoinduced ET process of (ZnP)–C₆₀/ITO. Further improvement of our C₆₀–metal cluster systems is under active investigation for the artificial photosynthetic applications.

Acknowledgment. The work at KAIST was supported by the NRL Program of the MOST of Korea and by the KOSEF (Project No. 1999-1-122-001-5). The work at Yonsei University was supported by the National Creative Research Initiatives Program of the KOSEF.

Supporting Information Available: Synthetic procedures of ZnP–C₆₀, photoelectrochemical data of (ZnP)–C₆₀/ITO, CVs of (ZnP)–C₆₀/ITO and related compounds in solution, AFM image, and fluorescence decay profiles of (ZnP)–C₆₀/ITO. This material is available free of charge via the Internet at <http://pubs.acs.org>.

References

- (a) Wasielewski, M. R. *Chem. Rev.* **1992**, *92*, 435–461. (b) Gust, D.; Moore, T. A.; Moore, A. L. *Acc. Chem. Res.* **2001**, *34*, 40–48.
- (a) Luo, C.; Guldi, D. M.; Maggini, M.; Menna, E.; Mondini, S.; Kotov, N. A.; Prato, M. *Angew. Chem., Int. Ed.* **2000**, *39*, 3905–3909. (b) Eckert, J.-F.; Nicoud, J.-F.; Nierengarten, J.-F.; Liu, S.-G.; Echegoyen, L.; Barigelli, F.; Armaroli, N.; Ouali, L.; Krasnikov, V.; Hadziioannou, G. *J. Am. Chem. Soc.* **2000**, *122*, 7467–7479. (c) Ikeda, A.; Hatano, T.; Shinkai, S.; Akiyama, T.; Yamada, S. *J. Am. Chem. Soc.* **2001**, *123*, 4855–4856. (d) Imahori, H.; Mori, Y.; Matano, Y. *J. Photochem. Photobiol. C* **2003**, *4*, 51–83.
- (a) Imahori, H.; Hagiwara, K.; Akiyama, T.; Aoki, M.; Taniguchi, S.; Okada, T.; Shirakawa, M.; Sakata, Y. *Chem. Phys. Lett.* **1996**, *263*, 545–550.
- (a) Cho, Y.-J.; Song, H.; Lee, K.; Kim, K.; Kwak, J.; Kim, S.; Park, J. T. *Chem. Commun.* **2002**, 2966–2967. (b) Lee, K.; Song, H.; Kim, B.; Park, J. T.; Park, S.; Choi, M.-G. *J. Am. Chem. Soc.* **2002**, *124*, 2872–2873. (c) Lee, G.; Cho, Y.-J.; Park, B. K.; Lee, K.; Park, J. T. *J. Am. Chem. Soc.* **2003**, *125*, 13920–13921. (d) Lee, K.; Song, H.; Park, J. T. *Acc. Chem. Res.* **2003**, *36*, 78–86.
- (a) O'Regan, B.; Grätzel, M. *Nature* **1991**, *353*, 737–740. (b) Kleverlaan, C. J.; Indelli, M. T.; Bignozzi, C. A.; Pavanin, L.; Scandola, F.; Hasselman, G. M.; Meyer, G. J. *J. Am. Chem. Soc.* **2000**, *125*, 2840–2849. (c) Yamada, H.; Imahori, H.; Nishimura, Y.; Yamazaki, I.; Ahn, T. K.; Kim, S. K.; Kim, D.; Fukuzumi, S. *J. Am. Chem. Soc.* **2003**, *125*, 9129–9139. (d) Imahori, H.; Kimura, M.; Hosomizu, K.; Sato, T.; Ahn, T. K.; Kim, S. K.; Kim, D.; Nishimura, Y.; Yamazaki, I.; Araki, Y.; Ito, O.; Fukuzumi, S. *Chem.–Eur. J.* **2004**, *10*, 5111–5122. (e) Guldi, D. M.; Zilbermann, I.; Anderson, G.; Li, A.; Balbinot, D.; Jux, N.; Hatzimarinaki, M.; Hirsch, A.; Prato, M. *Chem. Commun.* **2004**, 726–727.
- See Supporting Information.
- (a) Hunter, C. A.; Meah, M. N.; Sanders, J. K. M. *J. Am. Chem. Soc.* **1990**, *112*, 5773–5780. (b) Guldi, D. M.; Luo, C.; Da Ros, T.; Prato, M.; Diel, E.; Hirsch, A. *Chem. Commun.* **2000**, 375–376.
- Liu, S.; Lu, Y.; Kappes, M.; Ibers, J. A. *Science* **1991**, *254*, 408–410.
- Guldi, D. M. *Chem. Soc. Rev.* **2002**, *31*, 22–36.
- Shida, T. In *Electronic Absorption Spectra of Radical Ions*; Elsevier: Amsterdam, 1988; p 311.

JA044847X